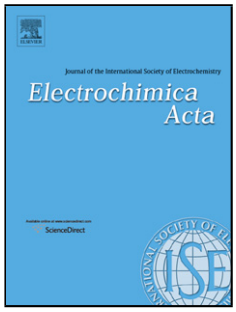

Title: Imparting improvements in electrochemical sensors: evaluation of different carbon blacks that give rise to significant improvement in the performance of electroanalytical sensing platforms<!–<query id="Q1"> “Your article is registered as a regular item and is being processed for inclusion in a regular issue of the journal. If this is NOT correct and your article belongs to a Special Issue/Collection please contact j.alwyn@elsevier.com immediately prior to returning your corrections.”</query>–>

Author: Fernando Campanhã Vicentini Amanda E. Ravanini Luiz C.S. Figueiredo-Filho Jesús Iniesta Craig E. Banks Orlando Fatibello-Filho

PII: S0013-4686(14)02489-X
DOI: http://dx.doi.org/doi:10.1016/j.electacta.2014.11.204
Reference: EA 23929

To appear in: *Electrochimica Acta*

Received date: 20-8-2014
Revised date: 21-10-2014
Accepted date: 12-11-2014

Please cite this article as: Fernando Campanhã Vicentini, Amanda E.Ravanini, Luiz C.S.Figueiredo-Filho, Jesús Iniesta, Craig E.Banks, Orlando Fatibello-Filho, Imparting improvements in electrochemical sensors: evaluation of different carbon blacks that give rise to significant improvement in the performance of electroanalytical sensing platforms, Electrochimica Acta http://dx.doi.org/10.1016/j.electacta.2014.11.204

Imparting improvements in electrochemical sensors: evaluation of different carbon blacks that give rise to significant improvement in the performance of electroanalytical sensing platforms

Fernando Campanhã Vicentini[a], *Amanda E. Ravanini*[a], *Luiz C. S. Figueiredo-Filho*[a], *Jesús Iniesta*[b], *Craig E. Banks*[c] *and Orlando Fatibello-Filho*[a]*

[a] Department of Chemistry, Federal University of São Carlos, Rod. Washington Luís km 235, P. O. Box 676, São Carlos, 13560-970, SP, Brazil.

[b]Physical Chemistry Department and Institute of Electrochemistry, University of Alicante, 03690 San Vicente del Raspeig, Alicante, Spain

[c] Faculty of Science and Engineering, School of Science and the Environment, Division of Chemistry and Environmental Science, Manchester Metropolitan University, Chester Street, Manchester M1 5GD, Lancs, UK.

* Corresponding author.

Tel.: +55 16 33518098; Fax: +55 16 33518350

E-mail address: bello@ufscar.br (O. Fatibello-Filho)

Graphical abstract

Abstract

Three different carbon black materials have been evaluated as a potential modifier, however, only one demonstrated an improvement in the electrochemical properties. The carbon black structures were characterised with SEM, XPS and Raman spectroscopy and found to be very similar to that of amorphous graphitic materials. The modifications utilised were constructed by three different strategies (using ultrapure water, chitosan and dihexadecylphosphate). The fabricated sensors are electrochemically characterised using N,N,N',N'-tetramethyl-para-phenylenediamine and both inner-sphere and outer-sphere redox probes, namely potassium ferrocyanide(II) and hexaammineruthenium(III) chloride, in addition to the biologically relevant and electroactive analytes, dopamine (DA) and acetaminophen (AP). Comparisons are made with an edge-plane pyrolytic graphite and glassy-carbon electrode and the benefits of carbon black implemented as a modifier for sensors within electrochemistry are explored, as well as the characterisation of their electroanalytical performances. We reveal significant improvements in the electrochemical performance (excellent sensitivity, faster heterogeneous electron transfer rate (HET)) over that of a bare glassy-carbon and edge-plane pyrolytic graphite electrode and thus suggest that there are substantial advantages of using carbon black as modifier in the fabrication of electrochemical based sensors. Such work is highly important and informative for those working in the field of electroanalysis where electrochemistry can provide portable, rapid, reliable and accurate sensing protocols (bringing the laboratory into the field), with particular relevance to those searching for new electrode materials.

Keywords: Carbon black; Advanced electrochemical materials; Chitosan; Electroanalysis.

1. Introduction

In the last decade, plenty of carbonaceous materials, such as, carbon nanofibers[1], carbon nanotube[2-5], graphene[6, 7], carbon black[8, 9], fulerenes[10, 11], carbon nanoparticles[12, 13] and carbonaceous foam materials[14] have been studied and used to develop new sensors and biosensors. Carbon black is generally used as inexpensive and high effectiveness reinforcement for rubber tyres and others polymer-matrix composites[15, 16] with its characteristics allowing carbon black to develop a fibrous morphology which exhibits a reinforcing ability. Also this material is applied as an electrically conductive filler in polymer-matrix composites[17-19] and this particular use calls attention to the development of electroanalytical sensors and other fields such as fuel cells and lithium batteries[20-22].

In terms of electrochemical performance, which corresponds to the key aims of this paper, until now very few applications are reported in the literature[9, 23-26] with the majority not explaining the behaviour and potentialities of carbon black. One notable contribution has been from Arduini *et al.*[8] who were the first to compare the electroanalytical performance of carbon black (CB N220) "film" deposited onto screen-printed electrodes with its electrochemical performance explored towards ferricyanide, epinephrine, norepinephrine, benzoquinone and NADH; their results shown significantly enhanced electrochemical activity when compared with screen-printed electrodes without the modification of carbon black. Following this notable work the same group presented two more electroanalytical applications of carbon black for metal determination (Hg^{2+}) where the authors reported a limit of detection of 5.0×10^{-9} mol L^{-1} and the proposed method was satisfactory applied for drinking waters with good recoveries[9] and was also used as a biosensor[27] platform/substrate to determine catechol using a tyrosinase enzyme reporting a low detection limit of 8.0×10^{-9} mol L^{-1}.

Note that in all these literature reports, no comparisons are made with a similar allotropic structures, that is, any other types of carbon blacks nor other graphitic electrodes; in this paper we make this key comparison, also in order to understand the behaviour of carbon black further, we make a critical comparison with edge-plane pyrolytic graphite allowing us to critically evaluate the electroanalytical performance of carbon blacks.

The development of new sensors with long shelf life's and improvements in electrochemical performance towards target analytes is not new with plenty of compounds reported to provide benefits such as through the additions of surfactants, polyelectrolytes and biopolymers onto electrode surfaces. For example, dihexadecylphosphate (DHP) is a hydrophobic surfactant which has two long hydrocarbon chains linked to a phosphate group that self-assemble into multiple bilayer structures similar to lipid bilayers and this structure allows stable films to be immobilised onto surface electrodes[28-30]. Also another common reticulant agent used is chitosan which produces films with high chemical stability and mechanical resistance; these chitosan films show other attractive characteristics such as excellent film-forming ability, high permeability, good adhesion, non-toxicity and susceptibility to various modifications with various chemical agents[31] and facilitates electron transfer due to their hydrophilic nature[32, 33].

Inspired by the limited amount of literature available on the highly fascinating carbon black within electrochemistry, we carried out careful experiments using carbon black as an electrode material towards commonly encountered redox probes in aqueous solutions, which also is contrasted to different types of carbon black and edge-plane pyrolytic graphite thus providing valuable information on the electronic properties and applicability of this intriguing material.

Additionally we perform experiments in order to demonstrate the electroanalytical performances of black carbon.

2. Experimental Section

Dihexadecylphosphate (DHP), chitosan (CTS) of low molecular weight and 80% deacetylation degree, potassium ferrocyanide(II), hexaammineruthenium(III) chloride, N,N,N',N'-tetramethyl-para-phenylenediamine (TMPD), dopamine (DA) and acetaminophen (AP) were purchased from Sigma-Aldrich. The VXC72R, BP4750 and E2000 carbon blacks (CBs) were kindly supplied by Cabot Corporation. All other chemicals were of analytical grade and were used as received without any further purification. A 1.0×10^{-3} mol L^{-1} DA and AP stock solutions were prepared in a 0.1 mol L^{-1} phosphate buffer solution (pH 7.0), which was made using NaH_2PO_4 and Na_2HPO_4. All solutions were prepared using nanopure water (resistivity > 18.2 MΩ cm) from Millipore Milli-Q system (Billerica, USA).

Voltammetric measurements were conducted using a model μAutolab type 3 potentiostat/galvanostat (Metrohm-Autolab, Utrecht, Netherlands) controlled by GPES 4.9 software. The voltammetric experiments were carried out with a three-electrode system: a platinum plate as counter electrode, an Ag/AgCl (3.0 mol L^{-1} KCl) as reference electrode to which all potentials are referred, and the working electrodes: a carbon black-modified glassy carbon electrode (CBs/GCE) (3 mm diameter), an edge-plane pyrolytic graphite (EPPG) electrode (Le Carbone, Ltd. Sussex, UK) was machined into a 4.9 mm diameter, with the disc face parallel to the edge plane as required from a slab of highly ordered pyrolytic graphite

(HOPG: highest grade available; SPI-1, equivalent to Union Carbide's ZYA grade, with a lateral grain size, L_a of 1–10 μm and 0.4 ± 0.1° mosaic spread) and a GCE (3 mm diameter) were also used. Cyclic voltammetric measurements were carried out in a 20.0 mL electrochemical cell. The background current was subtracted from all voltammograms. All experiments were carried out at room temperature (25 ± 1°C).

For SEM, Raman spectroscopy and XPS analysis, the respective powder was used as received from the supplier without any further modification. Scanning Electron Microscopy (SEM) images were obtained using a CB dispersion deposited over the GC surface, Supra 35-VP equipment (Carl Zeiss, Germany) with electron beam energy of 25 keV was employed. Raman spectra were recorded with all analyzes collected at a single point in the carbon blacks, which was performed using lens with 10x increase and 540 nm laser at a very low laser power level (0.9 mW) to avoid any heating effect at a dispersive Raman spectrometer Horiba / Join Yvon Labram equipped with an Olympus BX41 microscope (France) between 1000-4000 cm^{-1} and 10 seconds and 10 cycles of exposure. X-ray photoelectron spectroscopy (XPS, K-Alpha, Thermo Scientific) was used to analyse the respective powders. All spectra were collected using Al-K radiation (1486.6 eV), monochromatised by a twin crystal monochromator, yielding a focused X-ray spot with a diameter of 400 μm, at 3 mA × 12 kV. The alpha hemispherical analyser was operated in the constant energy mode with survey scan pass energies of 200 eV to measure the whole energy band and 50 eV in a narrow scan to selectively measure the particular elements. Thus, XPS was used to provide the chemical bonding state as well as the elemental composition of the powders utilised. Charge compensation was achieved with the system flood gun that provides low energy electrons and low energy argon ions from a single source.

Measurements of pH were performed using an Orion pH-meter, Expandable Ion Analyser, model EA-940, connected to a Digimed combined glass electrode.

2.1. Preparation of the CBs Dispersions

The CTS stock solution (1.0% w/w) was obtained as described previously[34]. Briefly, 0.5 g of CTS powder was dissolving in 50 mL of 1.0% (v/v) acetic acid solution at room temperature (25°C) and kept under constant stirring for 3 h until complete dissolution. The CTS stock solution was stored at 4°C in a refrigerator when not in use.

A GCE was carefully polished to a mirror finish with 0.3 and 0.05 μm alumina slurries, and rinsed thoroughly with ultrapure water. So, the GCE was sonicated in isopropyl alcohol and then with ultrapure water, each for about three minutes, and dried at room temperature.

Fig. 1 presents the strategies performed for preparation of the modified GCE with VXC72R CB within different films. The first strategy (dispersing in ultrapure water) was performed by ultrasonication of 1.0 mg of VXC72R CB in 1.0 mL of ultrapure water for 30 minutes. The second strategy (dispersing within DHP film) was prepared by ultrasonication of 1.0 mg of VXC72R CB and 1.0 mg of DHP in 1.0 mL of ultrapure water for 30 minutes to give a VXC72RCB-DHP suspension. The third strategy (dispersing within CTS film) was carried out by ultrasonication of 1.0 mg of CB in 1.0 mL of CTS stock solution (1.0% w/w) for 30 minutes to provide a VXC72RCB-CTS suspension. For each modified electrode, a volume of 8 μL of each suspension was dropped onto the GCE surface and the solvent allowed to evaporate for 2 h (at 25°C).

3. Results and Discussion

3.1. Physical Characterisation

We first consider the structural characterisation of the carbon black (CBs) samples, VXC72R, BP4750 and E2000, as can be observed in Table 1, XPS analysis was carried out to establish the elemental composition of each sample, where it can be readily observed that there is only a small difference between each sample. Furthermore, de-convolution of the spectra was conducted with this analysis revealing the VXC72R CB to be composed of 91.2 % carbon and 7.8 % oxygen. The carbon content comprises 74.35 % corresponding to 284.7 eV which is characteristic of graphitic groups, 10.66 % at 286 eV and 6.22 % at 289 eV which both correspond to C–O and C=O bonds respectively. The oxygen content is comprised from 3.7 % at 531.7 eV which corresponds to C–OH bonds and 4.1 % at 533.3 eV which corresponds to groups such as C=O, O=C–O, and C–O. Additionally, the XPS shows oxygenation in the carbon structure which was confirmed by Raman exhibiting a characteristic D band (see below).

Next, Raman spectroscopy was performed for all CBs (Fig. 2) which revealed two characteristic bands: D (1331 cm^{-1}) and G (1551 cm^{-1}) and a wide G' band at *ca.* 2800 cm^{-1}; which as reported widely in the literature is consistent with amorphous carbon materials[35-37]. The D band is usually attributed to the disorder and imperfection of the carbon crystallites (basal plane defects). The G band is assigned to one of the two E2g modes corresponding to stretching vibrations in the basal plane (sp^2 domains) of single crystal graphite or graphene[14]. The poor intensity G' band reveals that these materials present poor structural quality (closest to amorphous structure materials)[35]. Also as known, integrated intensity ratio ID/IG in the Raman spectrum should approximately correspond to the extent of order/disorder in the graphitic

carbon, in order to estimate the integrated intensity of D and G band was assumed as the full width at half maximum (FWHM) for the Lorentzian line [38], was carried out a comparison of the ID/IG ratio for the different carbon black in order to clarify the degree of order of carbon materials. The results showed a similar ratio for the two carbon blacks (VXC72R = 2.64 and E2000 = 2.36) and BP4750 CB presented a higher ratio value of 3.65. It should be pointed out that materials with R > 1, indicate that CBs are in the transition from graphite to nanocrystalline graphite [38]. For comparison, in the literature ratio values such as: a carbon nanofiber = 0.96 [39], vertically aligned carbon nanotubes = 0.54 and graphene oxide = 0.23 [40, 41] have been reported.

Finally, the CBs were analysed via SEM (see Fig. 3a-b for VXC72R CB, Fig. 3c for BP4750 CB and Fig. 3d for E2000 CB), which reveals a material consisting of multiple grains/nanoparticles of amorphous carbon, this nanoparticle material presents a high uniform size *c.a.* ~25 nm, probably due of the fabrication process. It is important to note that E2000 CB (Fig. 3d) shown a poor distribution over the GCE, leaving many uncovered areas. Moreover, this morphology results in a porous surface, which can provide a higher electroactive surface area. Also is evident from SEM images of VXC72R CB the nanoparticles do not exhibit a perfect spherical shape, there are wrinkles (as confirmed via Raman spectroscopy) over the surface which can potentially influence the electrochemical response and could give rise to beneficial electron transfer properties.

3.2. Electrochemistry Characterization

We first performed a study in order to produce a stable film over a glassy carbon (GCE) electrode substrate. VXC72R CB was suspended into ultrapure water with aliquots made onto

the GCE surface (see experimental section). Preliminary studies revealed a non-adherent film was produced and two well-known molecules were next evaluated: DHP and CTS in a proportion of 1 mg of VXC72RCB / (1 mL water or 1 mg DHP or 1mL CTS). As can be seen in Fig. 4, the VXC72RCB-CTS/GCE (black line) exhibits the greatest current with optimal voltammetric behaviour evident as observed through good electrochemical reversibility (close peak-to-peak separations) compared to the case of no CTS and a more adherent and stable (over 50 measurement with analytical signal ranging 4.2%) film. The VXC72RCB-DHP/GCE (blue line) shows good stability but appears to exhibit a less reversible electrochemical process. Thus, CTS was chosen for further experiments with the best proportion of CB optimised; VXC72RCB:CTS as 1.00 mg/mL (Fig. S1, in the Supporting Information) by varying the VXC72R CB proportion between 0.25 to 2.00 mg in a 1.0 mL of CTS stock solution (1.0% w/v).

We now turn to the electrochemical characterisation of our three carbon blacks (VXC72R CB, BP4750 CB and E2000 CB). This study was performed towards the well characterised inner-sphere redox probe ferro-/ferri- cyanide in 0.1 mol L^{-1} KCl. Fig. 5 shows typical voltammograms for VXC72RCB-CTS/GCE, BP4750CB-CTS/GCE and E2000CB-CTS/GCE at a scan rate of 100 mVs^{-1} exhibits a well-defined pair of redox peaks with a peak separation (ΔE_p) of *ca.* 215.3, 237.2 and 452.3mV (*vs*. Ag/AgCl (3.0 mol L^{-1} KCl)) for VXC72RCB-CTS/GCE, BP4750CB-CTS/GCE and E2000CB-CTS/GCE, respectively. The VXC72RCB-CTS/GCE and BP4750CB-CTS/GCE presents a small ΔE_p value than E2000CB-CTS/GCE, which is indicative of a more favourable electrochemical interaction at the electrode surface and thus enhanced electron transfer kinetics[42]. This worst voltammetric behaviour of E2000CB-CTS/GCE can be

attributed to the poor distribution of E2000CB over the GCE, as confirmed by the MEV (Fig. 3 (d)).

Scan rate studies were performed on the three different carbon blacks where the voltammetric peak height (I_p) was monitored as a function of scan rate (v) with a plot of peak height versus square-root of the scan rate revealing the following trends: VXC72RCB-CTS/GCE, I_p (A) = -4.91×10^{-6} A/$(Vs^{-1})^{0.5}$ + 1.58×10^{-4} A (R^2 = 0.998); BP4750CB-CTS/GCE, I_p (A) = 6.50×10^{-6} A/$(Vs^{-1})^{0.5}$ + 8.46×10^{-5} A (R^2 = 0.997); E2000CB-CTS/GCE, I_p (A) = 4.32×10^{-6} A/$(Vs^{-1})^{0.5}$ + 8.02×10^{-5} A (R^2 = 0.993). It is clear that in each of the cases a linear response is observed, indicating diffusional processes. Furthermore, an analysis of log I_p versus log v was carried out to be sure if the semi-infinite diffusion model was governed by the Randles–Ševćik equation[43], the gradients of 0.58 (VXC72RCB-CTS/GCE), 0.41 (BP4750CB-CTS/GCE) and 0.46 (E2000-CTS/GCE CB), indicate no thin-layer effects (such that the redox probe is not trapped within the network of the film) and representing a response that is purely diffusional in each case.

The most important parameter to evaluated the quality of an electrode material is the heterogeneous electron transfer (HET) rate (which is an advantageous characteristic in a plenty electrochemical areas)[42], which is intrinsically dependent of ΔE_P values, where a smaller ΔE_p value represents an increased reversibility of the redox probe utilised and thus faster HET kinetics at a given electrode material[7, 42].

For the inner-sphere redox probes performed, no significant changes was observed in the reversibility of the probe at two carbon blacks (VXC72RCB-CTS/GCE and BP4750CB-CTS/GCE), which exhibited similar ΔE_p values. However for E2000CB-CTS/GCE the ΔE_p value

was *ca*. 200 mV higher, note that inner-sphere redox mediators are strongly influenced/sensitive to the surface, where the state of the electrode surface (surface chemistry and microstructure) can give an improvement (or inhibition) via particular electro-catalytic interactions with specific surface oxygenated groups/species or impurities, such that the surface effects can strongly influence beneficially or detrimentally the electrochemical response[14, 42]. As presented in Table 1, the XPS analysis shows a high concentration of Ni in the E2000 carbon black structure, which probably gives a detrimental response for HET [44].

Returning to the electrochemical comparison of the carbon blacks, attention was turned to exploring the performance towards the outer-sphere electron transfer redox probe 1 mmol L^{-1} hexaammineruthenium(III) chloride in 0.1 mol L^{-1} KCl, the voltammetric behaviour of the three carbon blacks electrodes was recorded and found to exhibit reversible profiles (Fig. S2, in the Supporting Information). Similarly to the ferro/ferri probe the (ΔE_p) showed a small variance between the values obtained (*ca*. 63.4, 66.5 and ca. 68.7 mV for VXC72RCB-CTS/GCE, BP4750CB-CTS/GCE and E2000CB-CTS/GCE respectively at a scan rate of 100 mVs^{-1} (vs. 3.0 mol L^{-1} Ag/AgCl).

In the case of an outer-sphere probe the electrochemical response is sensitive to the electronic structure of the electrode material (the respective coverage of 'reactive' edge plane sites or 'un-reactive' basal plane sites, for the case of graphitic materials),[14, 42, 45]. For the outer-sphere system the electrode acts solely as an electron sink/supplier and electron transfer is not influenced by the surface state (absence/presence of specific oxygen containing functionalities, or the surface cleanliness in terms of the presence of uncharged impurities)[7, 42]. The insights gained above indicate that the three CBs exhibit similar electronic structures (once no significant changes was observed).

In order to estimate the heterogeneous electron transfer rate constant, k^0, was used the outer-sphere electron transfer probe hexaammineruthenium(III) chloride. The Nicholson method was applied to estimate the observed standard HET rate constant (k^0) for quasi-reversible systems using the following equation[46]:

$$\Psi = k^0 \left[\pi D n \omega F / (RT)\right]^{-1/2}$$

where Ψ a the kinetic parameter, D is the diffusion coefficient, n is the number of electrons involved in the process, F is the Faraday constant, R the gas constant and T the temperature. The kinetic parameter, Ψ, is tabulated as a function of ΔE_p at a set temperature (298 K) for a one-step, one electron process (where the transfer coefficient, $\alpha = 0.5$)[46]. The function of Ψ (ΔE_p), which fits Nicholson's data, for practical usage (rather than producing a working curve) is given by:

$$\Psi = (-0.6288 + 0.0021X) / (1 - 0.017X)$$

where $X = \Delta E_p$ is used to determine Ψ as a function of ΔE_p from the experimentally recorded voltammetry. From this, a plot of Ψ against (scan rate$^{-1/2}$ × 32.79) allows the k^0 to be readily determined. Using this approach the k^0 values of 9.26×10^{-2}, 5.74×10^{-3} and 6.23×10^{-4} cm s^{-1} were estimated for the for VXC72RCB-CTS/GCE, BP4750CB-CTS/GCE and E2000CB-CTS/GCE respectively (utilising a D of 9.1×10^{-6} cm^2 s^{-1} for hexaammineruthenium(III) chloride[47, 48] in 0.1 mol L^{-1} KCl and deduced over the scan rate range of 5–500 mV s^{-1}). The obtained k^0 value for VXC72R CB was 160 higher than for a fluorinated tin oxide glass electrode (FTO) modified with single-walled carbon nanotubes (SWCNT) (5.76×10^{-4} cm s^{-1}) and 153

higher than FTO modified with double-walled carbon nanotubes (DWCNT) as presented by Moore *et al.*[49] which also used the hexaammineruthenium(III) chloride probe. This result confirms the great ability of the VXC72RCB-CTS/GCE to transfer electrons. The next step was analysis of the anodic peak against square-root of the scan rate, where all equations present linear response, indicating clearly a diffusional process (again indicating no possibility of the electroactive analyte being trapped inside of the film/structure).

Next we turn to exploring the voltammetry of N,N,N',N'-tetramethyl-para-phenylenediamine (TMPD). The VXC72RCB-CTS/GCE cyclic voltammograms (CV) show a higher current, better voltammetric profile and an improvement in its electrochemical reversibility over the others alternatives (BP4750CB-CTS/GCE and E2000CB-CTS/GCE), in terms of HET kinetics, as deduced through the ΔE_p values for the first and second redox peak-couples (*ca.* 56.9 and 79.9 (at VXC72RCB-CTS/GCE), 58.0 and 97.2 mV (BP4750CB-CTS/GCE) and 88.6 and 106.2 mV (E2000CB-CTS/GCE), at 50 mVs^{-1}). Fig. 6 shows the CVs obtained with CB's-CTS/GCE. Note that (as discussed earlier) in all cases, diffusional processes are in operation. Is well known[50, 51] the electrochemical process at TMPD, which is due to two one-electron oxidations (and corresponding reductions on the reverse scan), described as:

$$TMPD - e^- \longrightarrow TMPD^{\bullet+}$$
$$TMPD^{\bullet+} - e \longrightarrow TMPD^{2+}$$

which gives rise to the unique voltammetric profiles observed in Fig. 6. At this point it is worth considering the origin of the observed electrochemical responses. From inspection of the XPS data, it is clear that E2000 CB has the greatest amount of nickel, followed by VXC72R CB and then BP4750 CB. If the origin of the electrochemical responses above were soley due to the occluded nickel, then we would expect E2000CB-CTS/GCE to consistently give rise to the best

voltammetric responses which is not the case but rather VXC72CB-CTS/GCE does. The nickel, due to the fabrication process of the carbon black resides as an oxide and hence its electrochemical activity is reduced/ negligible. While metals in carbon black samples cannot be one hundred percent excluded, that is, they are always present in such samples, it is good practice to consider exactly what the origin of the observed electrochemical response is.

3.3. Electroanalytical Applications

Following the morphological and electrochemistry characterisations as described above, we start exploring the electroanalytical response for AP using the VXC72RCB-CTS/GCE, EPPG and GCE via cyclic voltammetry. Fig. 7 (a) shows the voltammetric responses obtained which indicate that VXC72RCB-CTS/GCE presents a smaller peak-to-peak separation (*ca*. 393.0 mV) when compared with the others electrodes (*ca*. 485.1 mV for EPPG and 500.2 mV GCE), after was carried out successive additions of AP into a 0.1 mol L^{-1} phosphate buffer solution, pH 7.0. Fig. 7 (b) shows the response of analytical signal (cathodic current density) (j) as a function of AP concentration. It is clear that linear responses are observed over the concentration range studied, 2.5×10^{-6} to 9.0×10^{-5} mol L^{-1}, however it is most remarkable the VXC72RCB-CTS/GCE exhibits an improvement over that of EPPG in terms of the observed sensitivity (slope of the calibration plot); usually EPPG shows the best sensitivity among different carbonaceous materials as can found in the literature[6, 52, 53]. The linear equations for the electroanalytical response using VXC72RCB-CTS/GCE are as follows: j (μAcm^{-2}) = 4.36×10^{-6} + 0.60 ([AP] $\mu mol\ L^{-1}$), R^2 = 0.997; j (μAcm^{-2}) = -7.15×10^{-7} + 0.29 ([AP] $\mu mol\ L^{-1}$), R^2 = 0.999 for the EPPG and j (μAcm^{-2}) = -5.13×10^{-7} + 0.22 ([AP] $\mu mol\ L^{-1}$), R^2 = 0.999) for the GCE.

Fig. 8 explores the electrochemistry of DA; note DA is a catecholamine neurotransmitter that has vital function of the hormonal, renal and central nervous systems. However, abnormal DA concentrations have been associated with neurological disorders; thus, the determination of the DA concentration can be very important in diagnostic applications[7, 54]. As shown in Fig. 8 (a), the cyclic voltammograms (Fig. 7 (a)) give no significant changes to an oxidation peak at *ca.* 0.198, 0.209 and 0.230 V at the VXC72RCB-CTS/GCE, EPPG and GCE respectively (50 mVs^{-1}).

We turn to exploring the electroanalytical response from successive additions of DA into a 0.1 mol L^{-1} phosphate buffer solution, pH 7.0 using VXC72RCB-CTS/GCE, EPPG and GCE, which is presented in Fig. 8 (b) with the appropriate calibration plots. It is evident that the linear response for VXC72RCB-CTS/GCE exhibits a better sensitivity, with a linear equation j (μAcm^{-2}) = 3.57×10^{-6} + 0.53 ([DA] µmol L^{-1}), R^2 = 0.999, when contrasted with EPPG (j (μAcm^{-2}) = 1.18×10^{-6} + 0.36 ([DA] µmol L^{-1}), R^2 = 0.996) and GCE (j (μAcm^{-2}) = 5.82×10^{-7} + 0.15 ([DA] µmol L^{-1}), R^2 = 0.999). Although, the linear range was lower for VXC72RCB-CTS/GCE, this can be attributed to the large background current (Fig. S3, in the Supporting Information), that is evident when utilising this electrode, however, as with each of the previous analytes it is clear that the analytical sensitivity of the VXC72RCB-CTS/GCE is greater than others graphitic electrodes.

Table 2 summarises the analytical performance of the carbon based electrodes in terms of the sensitivity (Acm^{-2} L mol^{-1}) and detection limits (mol L^{-1}) (three times the standard deviation of the blank solution divided by the slope of the analytical curve) towards the AP and DA.

Inspection of Table 2 indicates that VXC72RCB-CTS/GCE exhibits the highest sensitivity and lowest detection limits than that achievable using the EPPG or GCE. The intra-day repeatability of the VXC72RCB-CTS/GCE, EPPG and GCE were determined for 9.9×10^{-6} mol L^{-1} AP and DA solutions in 0.1 mol L^{-1} phosphate buffer solution, pH 7.0. The relative standard deviation (RSD) values obtained were 2.35%, 2.77% and 3.17% for AP and 0.51%, 1.44% and 2.63% for DA; (N = 5, VXC72RCB-CTS/GCE, EPPG and GCE, respectively), indicating a good stability of the VXC72RCB-CTS film. Given the results and discussion above, it appears that there is apparent advantage of using VXC72RCB as modifier for electrodes for the electroanalysis of target analytes in aqueous based solutions.

4. Conclusions

This work demonstrates the potential of VXC72R CB as electrode modifier which is shown to consistently out-perform routinely used alternatives in terms of both electron transfer kinetics (HET rates) and the magnitude of the analytically important current passed in all instances, between all the carbon blacks used as comparison. The morphological characterization was fully investigated and the results demonstrate the difference of VXC72R CB between others carbon blacks (BP4750 and E2000) indicating a promising platform from which the development of next generation electrochemical sensors.

Acknowledgments

The authors acknowledge financial support from the following Brazilian funding agencies: FAPESP (Proc. 2013/16770-0, 2014/04284-6 and 2010/20754-1), CNPq and CAPES.

References

[1] L. Wu, X.J. Zhang, H.X. Ju, Amperometric glucose sensor based on catalytic reduction of dissolved oxygen at soluble carbon nanofiber, Biosens. Bioelectron., 23 (2007) 479-484.
[2] C.X. Cai, J. Chen, Direct electron transfer of glucose oxidase promoted by carbon nanotubes, Anal. Biochem., 332 (2004) 75-83.
[3] C.E. Banks, T.J. Davies, G.G. Wildgoose, R.G. Compton, Electrocatalysis at graphite and carbon nanotube modified electrodes: edge-plane sites and tube ends are the reactive sites, Chem. Commun., (2005) 829-841.
[4] G.G. Oliveira, D.C. Azzi, F.C. Vicentini, E.R. Sartori, O. Fatibello-Filho, Voltammetric determination of verapamil and propranolol using a glassy carbon electrode modified with functionalized multiwalled carbon nanotubes within a poly (allylamine hydrochloride) film, J. Electroanal. Chem., 708 (2013) 73-79.
[5] F.C. Vicentini, L.C.S. Figueiredo-Filho, B.C. Janegitz, A. Santiago, E.R. Pereira-Filho, O. Fatibello-Filho, Factorial design and response surface: voltammetric method optimization for the determination of Ag(I) employing a carbon nanotubes paste electrode, Quim. Nova, 34 (2011) 825-830.
[6] L.C.S. Figueiredo-Filho, D.A.C. Brownson, O. Fatibello-Filho, C.E. Banks, Exploring the origins of the apparent "electrocatalytic" oxidation of kojic acid at graphene modified electrodes, Analyst, 138 (2013) 4436-4442.
[7] L.C.S. Figueiredo-Filho, D.A.C. Brownson, M. Gomez-Mingot, J. Iniesta, O. Fatibello-Filho, C.E. Banks, Exploring the electrochemical performance of graphitic paste electrodes: graphene vs. graphite, Analyst, 138 (2013) 6354-6364.
[8] F. Arduini, F. Di Nardo, A. Amine, L. Micheli, G. Palleschi, D. Moscone, Carbon Black-Modified Screen-Printed Electrodes as Electroanalytical Tools, Electroanalysis, 24 (2012) 743-751.
[9] F. Arduini, C. Majorani, A. Amine, D. Moscone, G. Palleschi, Hg2+ detection by measuring thiol groups with a highly sensitive screen-printed electrode modified with a nanostructured carbon black film, Electrochim. Acta, 56 (2011) 4209-4215.
[10] Z.L. Wei, Z.J. Li, X.L. Sun, Y.J. Fang, J.K. Liu, Synergistic contributions of fullerene, ferrocene, chitosan and ionic liquid towards improved performance for a glucose sensor, Biosens. Bioelectron., 25 (2010) 1434-1438.
[11] S.S. Kalanur, S. Jaldappagari, S. Balakrishnan, Enhanced electrochemical response of carbamazepine at a nano-structured sensing film of fullerene-C-60 and its analytical applications, Electrochim. Acta, 56 (2011) 5295-5301.
[12] M. Ghalkhani, S. Shahrokhian, Application of carbon nanoparticle/chitosan modified electrode for the square-wave adsorptive anodic striping voltammetric determination of Niclosamide, Electrochem. Commun., 12 (2010) 66-69.
[13] B.J. Sanghavi, G. Hirsch, S.P. Karna, A.K. Srivastava, Potentiometric stripping analysis of methyl and ethyl parathion employing carbon nanoparticles and halloysite nanoclay modified carbon paste electrode, Anal. Chim. Acta, 735 (2012) 37-45.
[14] D.A.C. Brownson, L.C.S. Figueiredo-Filho, X.B. Ji, M. Gomez-Mingot, J. Iniesta, O. Fatibello-Filho, D.K. Kampouris, C.E. Banks, Freestanding three-dimensional graphene foam gives rise to beneficial electrochemical signatures within non-aqueous media, J. Mater. Chem. A, 1 (2013) 5962-5972.

[15] A. Mostafa, A. Abouel-Kasem, M.R. Bayoumi, M.G. El-Sebaie, Rubber-Filler Interactions and Its Effect in Rheological and Mechanical Properties of Filled Compounds, J. Test. Eval., 38 (2010) 347-359.
[16] M. Gerspacher, Advanced CB Characterizations to Better Understand Polymer-Filler Interaction A Critical Survey, KGK-Kautsch. Gummi Kunstst., 62 (2009) 233-239.
[17] J.-C. Huang, Carbon black filled conducting polymers and polymer blends, Advances in Polymer Technology, 21 (2002) 299-313.
[18] F. Carmona, J. Ravier, Electrical properties and mesostructure of carbon black-filled polymers, Carbon, 40 (2002) 151-156.
[19] N. Probst, C. Van Bellingen, H. Van den Bergh, Compounding with conductive carbon black, Plastics, Additives and Compounding, 11 (2009) 24-27.
[20] A.R. Hopkins, N.S. Lewis, Detection and classification characteristics of arrays of carbon black/organic polymer composite chemiresistive vapor detectors for the nerve agent simulants dimethylmethylphosphonate and diisopropylmethylphosponate, Anal. Chem., 73 (2001) 884-892.
[21] R. Alcantara, J.M. Jimenez-Mateos, P. Lavela, J.L. Tirado, Carbon black: a promising electrode material for sodium-ion batteries, Electrochem. Commun., 3 (2001) 639-642.
[22] R. Dominko, M. Gaberscek, J. Drofenik, M. Bele, J. Jamnik, Influence of carbon black distribution on performance of oxide cathodes for Li ion batteries, Electrochim. Acta, 48 (2003) 3709-3716.
[23] F. Arduini, A. Amine, C. Majorani, F. Di Giorgio, D. De Felicis, F. Cataldo, D. Moscone, G. Palleschi, High performance electrochemical sensor based on modified screen-printed electrodes with cost-effective dispersion of nanostructured carbon black, Electrochem. Commun., 12 (2010) 346-350.
[24] A. Liberti, C. Morgia, M. Mascini, Graphitized carbon-black in polyethylene as an electrochemical sensor, Anal. Chim. Acta, 173 (1985) 157-164.
[25] S.B. Hocevar, B. Ogorevc, Preparation and characterization of carbon paste micro-electrode based on carbon nano-particles, Talanta, 74 (2007) 405-411.
[26] I.G. Svegl, M. Bele, B. Ogorevc, Carbon black nanoparticles film electrode prepared by using substrate-induced deposition approach, Anal. Chim. Acta, 628 (2008) 173-180.
[27] F. Arduini, F. Di Giorgio, A. Amine, F. Cataldo, D. Moscone, G. Palleschi, Electroanalytical characterization of carbon black nanomaterial paste electrode: development of highly sensitive tyrosinase biosensor for catechol detection, Anal. Lett., 43 (2010) 1688-1702.
[28] D. Asbahr, L.C.S. Figueiredo-Filho, F.C. Vicentini, G.G. Oliveira, O. Fatibello-Filho, C.E. Banks, Differential pulse adsorptive stripping voltammetric determination of nanomolar levels of methotrexate utilizing bismuth film modified electrodes, Sens. Actuator B-Chem., 188 (2013) 334-339.
[29] L.L.C. Garcia, L.C.S. Figueiredo-Filho, G.G. Oliveira, O. Fatibello-Filho, C.E. Banks, Square-wave voltammetric determination of paraquat using a glassy carbon electrode modified with multiwalled carbon nanotubes within a dihexadecylhydrogenphosphate (DHP) film, Sens. Actuator B-Chem., 181 (2013) 306-311.
[30] F.C. Vicentini, B.C. Janegitz, C.M.A. Brett, O. Fatibello-Filho, Tyrosinase biosensor based on a glassy carbon electrode modified with multi-walled carbon nanotubes and 1-butyl-3-methylimidazolium chloride within a dihexadecylphosphate film, Sens. Actuator B-Chem., 188 (2013) 1101-1108.

[31] K.V.H. Prashanth, R.N. Tharanathan, Chitin/chitosan: modifications and their unlimited application potential - an overview, Trends Food Sci. Technol., 18 (2007) 117-131.
[32] B. Batra, C.S. Pundir, An amperometric glutamate biosensor based on immobilization of glutamate oxidase onto carboxylated multiwalled carbon nanotubes/gold nanoparticles/chitosan composite film modified Au electrode, Biosens. Bioelectron., 47 (2013) 496-501.
[33] B.C. Janegitz, L.H. Marcolino-Junior, S.P. Campana, R.C. Faria, O. Fatibello-Filho, Anodic stripping voltammetric determination of copper(II) using a functionalized carbon nanotubes paste electrode modified with crosslinked chitosan, Sens. Actuator B-Chem., 142 (2009) 260-266.
[34] R. Pauliukaite, M.E. Ghica, O. Fatibello-Filho, C.M.A. Brett, Electrochemical impedance studies of chitosan-modified electrodes for application in electrochemical sensors and biosensors, Electrochim. Acta, 55 (2010) 6239-6247.
[35] A.V. Baranov, A.N. Bekhterev, Y.S. Bobovich, V.I. Petrov, Interpretation of some singularities in Raman-specta of graphite and glass carbon, Opt. Spektrosk., 62 (1987) 1036-1042.
[36] M.I. Nathan, J.E. Smith, K.N. Tu, Raman-spectra of glassy carbon, J. Appl. Phys., 45 (1974) 2370-2370.
[37] J. Schwan, S. Ulrich, V. Batori, H. Ehrhardt, S.R.P. Silva, Raman spectroscopy on amorphous carbon films, J. Appl. Phys., 80 (1996) 440-447.
[38] A.C. Ferrari, J. Robertson, Interpretation of Raman spectra of disordered and amorphous carbon, Phys. Rev. B, 61 (2000) 14095-14107.
[39] E. Enríquez, J. de Frutos, J.F. Fernández, M.A. de la Rubia, Conductive coatings with low carbon-black content by adding carbon nanofibers, Composites Science and Technology, 93 (2014) 9-16.
[40] T.A. Silva, H. Zanin, E. Saito, R.A. Medeiros, F.C. Vicentini, E.J. Corat, O. Fatibello-Filho, Electrochemical behaviour of vertically aligned carbon nanotubes and graphene oxide nanocomposite as electrode material, Electrochim. Acta, 119 (2014) 114-119.
[41] J. Kastner, T. Pichler, H. Kuzmany, S. Curran, W. Blau, D.N. Weldon, M. Delamesiere, S. Draper, H. Zandbergen, Resonance Raman and infrared spectroscopy of carbon nanotubes, Chemical Physics Letters, 221 (1994) 53-58.
[42] D.A.C. Brownson, D.K. Kampouris, C.E. Banks, Graphene electrochemistry: fundamental concepts through to prominent applications, Chem. Soc. Rev., 41 (2012) 6944-6976.
[43] S.J. Konopka, B. McDuffie, Diffusion coefficients of ferricyanide and ferrocyanide ions in aqueous media, using twin-electrode thin-layer electrochemistry, Anal. Chem., 42 (1970) 1741-&.
[44] S.M. Tan, A. Ambrosi, B. Khezri, R.D. Webster, M. Pumera, Towards electrochemical purification of chemically reduced graphene oxide from redox accessible impurities, Phys. Chem. Chem. Phys., 16 (2014) 7058-7065.
[45] T.J. Davies, M.E. Hyde, R.G. Compton, Nanotrench arrays reveal insight into graphite electrochemistry, Angew. Chem.-Int. Edit., 44 (2005) 5121-5126.
[46] R.S. Nicholson, Theory and application of cyclic voltammetry for measurement of electrode reaction kinetics, Anal. Chem., 37 (1965) 1351-&.
[47] T.J. Meyer, H. Taube, Electron-transfer reaction of ruthenium ammines, Inorg. Chem., 7 (1968) 2369-&.
[48] E.J.F. Dickinson, J.G. Limon-Petersen, N.V. Rees, R.G. Compton, How Much Supporting Electrolyte Is Required to Make a Cyclic Voltammetry Experiment Quantitatively "Diffusional"? A Theoretical and Experimental Investigation, J. Phys. Chem. C, 113 (2009) 11157-11171.

[49] K.E. Moore, B.S. Flavel, A.V. Ellis, J.G. Shapter, Comparison of double-walled with single-walled carbon nanotube electrodes by electrochemistry, Carbon, 49 (2011) 2639-2647.
[50] R.G. Evans, O.V. Klymenko, C. Hardacre, K.R. Seddon, R.G. Compton, Oxidation of N,N,N ',N '-tetraalkyl-para-phenylenediamines in a series of room temperature ionic liquids incorporating the bis(trifluoromethylsulfonyl)imide anion, J. Electroanal. Chem., 556 (2003) 179-188.
[51] R.G. Evans, O.V. Klymenko, P.D. Price, S.G. Davies, C. Hardacre, R.G. Compton, A comparative electrochemical study of diffusion in room temperature ionic liquid solvents versus acetonitrile, ChemPhysChem, 6 (2005) 526-533.
[52] D.A.C. Brownson, A.C. Lacombe, M. Gomez-Mingot, C.E. Banks, Graphene oxide gives rise to unique and intriguing voltammetry, RSC Advances, 2 (2012) 665-668.
[53] D.A.C. Brownson, C.E. Banks, Graphene electrochemistry: an overview of potential applications, Analyst, 135 (2010) 2768-2778.
[54] R.A. Medeiros, R. Matos, A. Benchikh, B. Saidani, C. Debiemme-Chouvy, C. Deslouis, R.C. Rocha-Filho, O. Fatibello-Filho, Amorphous carbon nitride as an alternative electrode material in electroanalysis: Simultaneous determination of dopamine and ascorbic acid, Anal. Chim. Acta, 797 (2013) 30-39.

Figure Captions

Fig. 1. Schematic representation of the GCE modification.

Fig. 2. Raman spectra of (a) VXC72R CB, (b) BP4750 CB and (c) E2000 CB.

Fig. 3. SEM images of (a – b) VXC72R CB, (c) BP4750 CB and (d) E2000 CB on the surface of GCE at different magnifications: (a) 40,000 × (b, c and d) 250,000 ×.

Fig. 4. Cyclic voltammetric of 1.0×10^{-3} mol L^{-1} potassium ferrocyanide(II) in 0.1 mol L^{-1} KCl recorded on VXC72RCB-CTS/GCE (black line), VXC72RCB-water/GCE (red line) and VXC72RCB-DHP/GCE (blue line) at scan rate 25 mV s^{-1}.

Fig. 5. Cyclic voltammetric profiles of VXC72RCB-CTS/GCE (black line), BP4750CB-CTS/GCE (red line) and E2000CB-CTS/GCE (blue line) recorded towards 1.0×10^{-3} mol L^{-1} potassium ferrocyanide(II) in 0.1 mol L^{-1} KCl, v = 100 mV s^{-1}.

Fig. 6. Cyclic voltammetric profiles of VXC72RCB-CTS/GCE (black line), BP4750CB-CTS/GCE (red line) and E2000CB-CTS/GCE (blue line), recorded towards 1.0×10^{-3} mol L^{-1} TMPD in 0.1 mol L^{-1} KCl, v = 50 mV s^{-1}.

Fig. 7. (a) Cyclic voltammetric profiles of VXC72RCB-CTS/GCE (black line), EPPG (red line) and GCE (blue line), recorded towards 5.21×10^{-5} mol L^{-1} AP in 0.1 mol L^{-1} phosphate buffer solution, pH 7.0, v = 50 mV s^{-1}. (b) Calibration plot after successive additions of AP for VXC72RCB-CTS/GCE (black squares), EPPG (red circles) and GCE (blue triangles).

Fig. 8. (a) Cyclic voltammetric profiles of VXC72RCB-CTS/GCE (black line), EPPG (red line) and GCE (blue line), recorded towards 5.21×10^{-5} mol L^{-1} DA in 0.1 mol L^{-1} phosphate buffer

solution, pH 7.0, v = 50 mV s^{-1}. (b) Calibration plot after successive additions of DA for VXC72RCB-CTS/GCE (black squares), EPPG (red circles) and GCE (blue triangles).

Table 1

Atomic weight percentage obtained from the XPS.

Sample	**Carbon**		**Oxygen**		**Sulphur**		**Nickel**	
	Binding energy	wt%	Binding energy	wt%	Binding energy	wt%	Binding energy	wt%
VXC72R CB	284.73 286.52 289.03	74.35 10.66 6.22	532.14 533.57	3.73 4.11	163.71 164.77	0.23 0.23	399.75 400.57	0.32 0.15
BP4750 CB	284.73 286.51 289.03	74.07 10.81 6.43	532.14 533.56	3.8 4.12	163.53 164.79	0.24 0.24	399.38 400.56	0.1 0.2
E2000 CB	284.88 286.68 288.90	72.2 7.92 6.64	532.06 533.55	6.33 5.52	163.36 164.58 167.71 168.85	0.16 0.16 0.24 0.24	399.74 400.65	0.5 0.09

N = 3

Table 2

Comparison of the analytical parameters for determination of AP and DA using VXC72RCB-CTS/GCE, EPPG and GCE electrodes using CV.

Analyte	Electrode	Analytical parameter	Obtained values
AP	VXC72RCB-CTS/GCE	Sensitivity (Acm^{-2} L mol^{-1})	0.60
		Detection limit (mol L^{-1})	1.9×10^{-7}
		Linear range (mol L^{-1})	5.0×10^{-6} to 9.0×10^{-5}
	EPPG	Sensitivity (Acm^{-2} L mol^{-1})	0.29
		Detection limit (mol L^{-1})	3.6×10^{-7}
		Linear range (mol L^{-1})	2.5×10^{-6} to 9.0×10^{-5}
	GCE	Sensitivity (Acm^{-2} L mol^{-1})	0.22
		Detection limit (mol L^{-1})	5.0×10^{-7}
		Linear range (mol L^{-1})	2.5×10^{-6} to 9.0×10^{-5}

DA	VXC72RCB-CTS/GCE	Sensitivity (Acm^{-2} L mol^{-1})	0.53
		Detection limit (mol L^{-1})	2.1×10^{-7}
		Linear range (mol L^{-1})	5.0×10^{-6} to 9.0×10^{-5}
	EPPG	Sensitivity (Acm^{-2} L mol^{-1})	0.36
		Detection limit (mol L^{-1})	5.6×10^{-7}
		Linear range (mol L^{-1})	2.5×10^{-6} to 9.0×10^{-5}
	GCE	Sensitivity (Acm^{-2} L mol^{-1})	0.15
		Detection limit (mol L^{-1})	1.0×10^{-6}
		Linear range (mol L^{-1})	2.5×10^{-6} to 9.0×10^{-5}

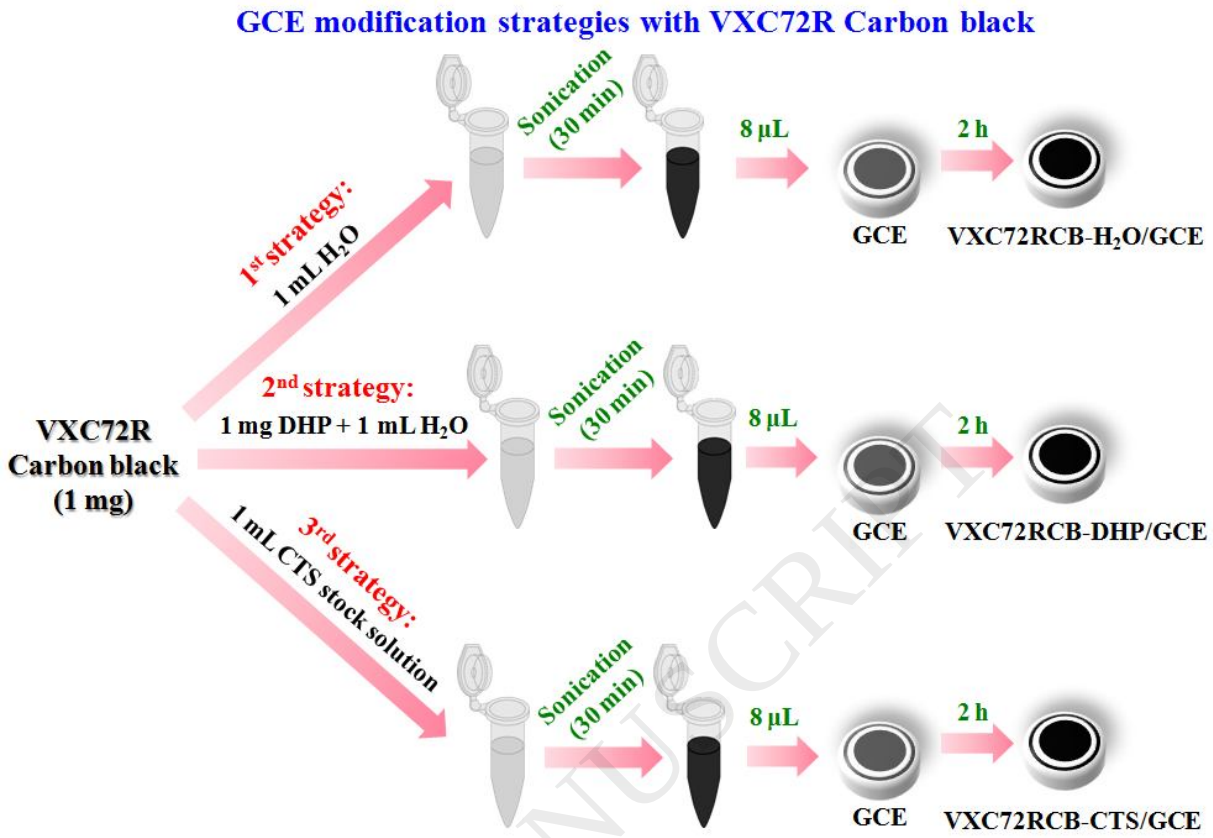

Fig 1 .

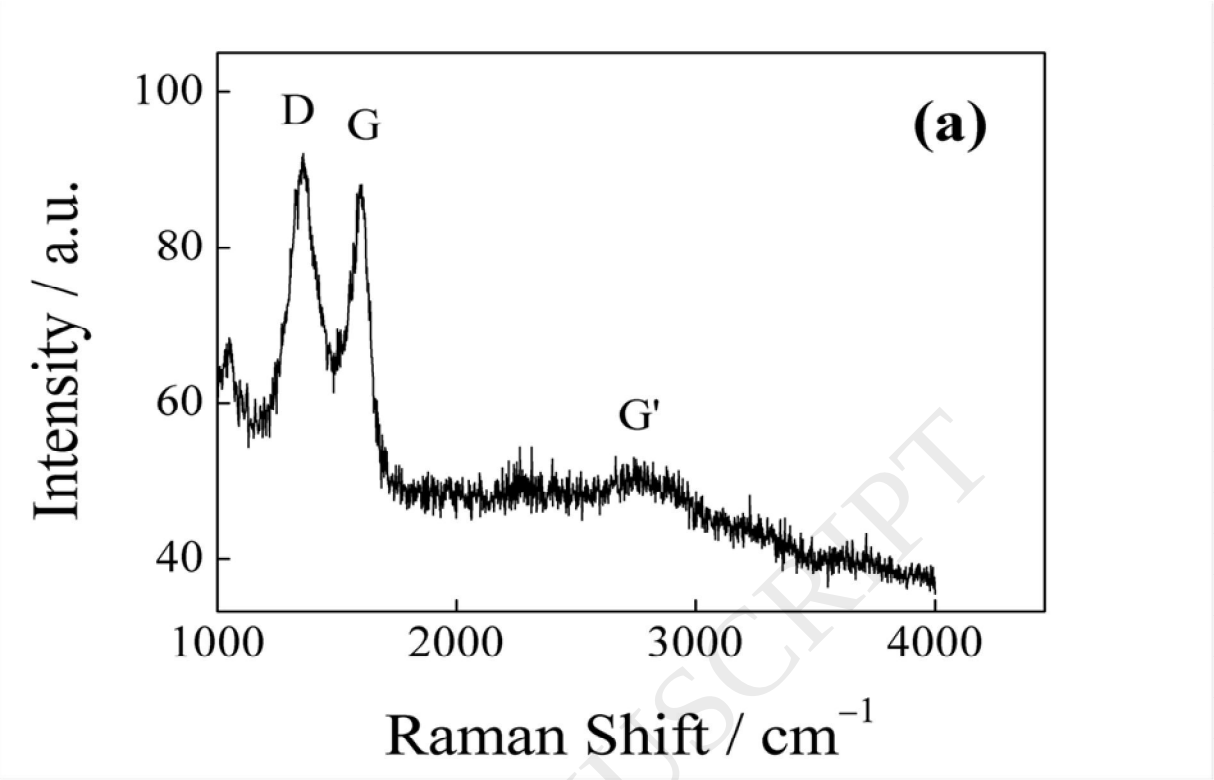

Fig 2 (a) .

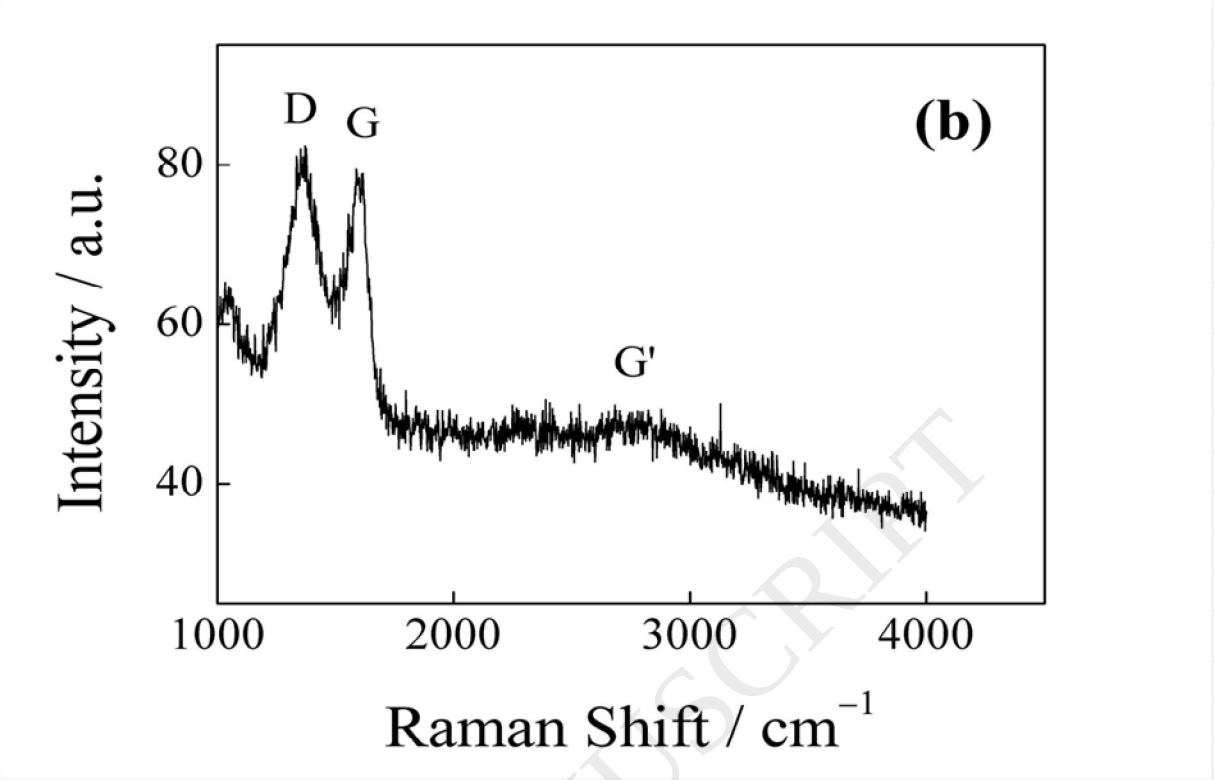

Fig 2 (b) .

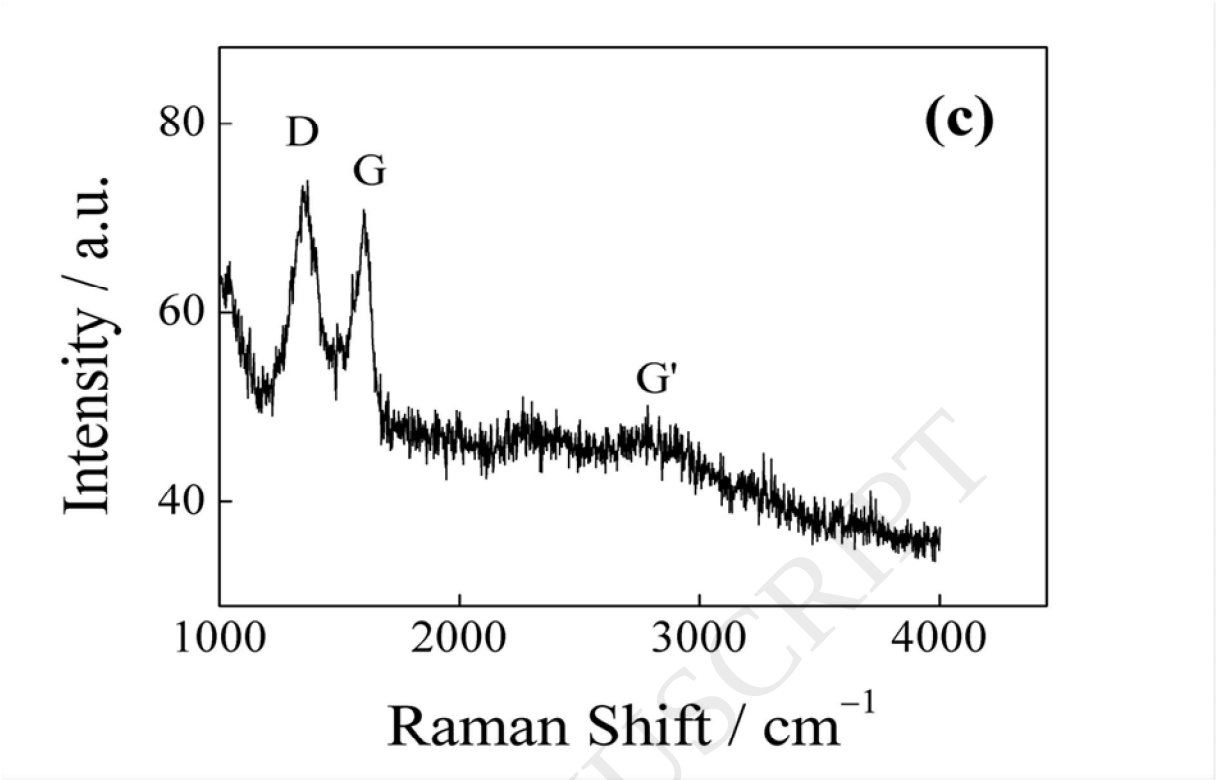

Fig 2 (c) .

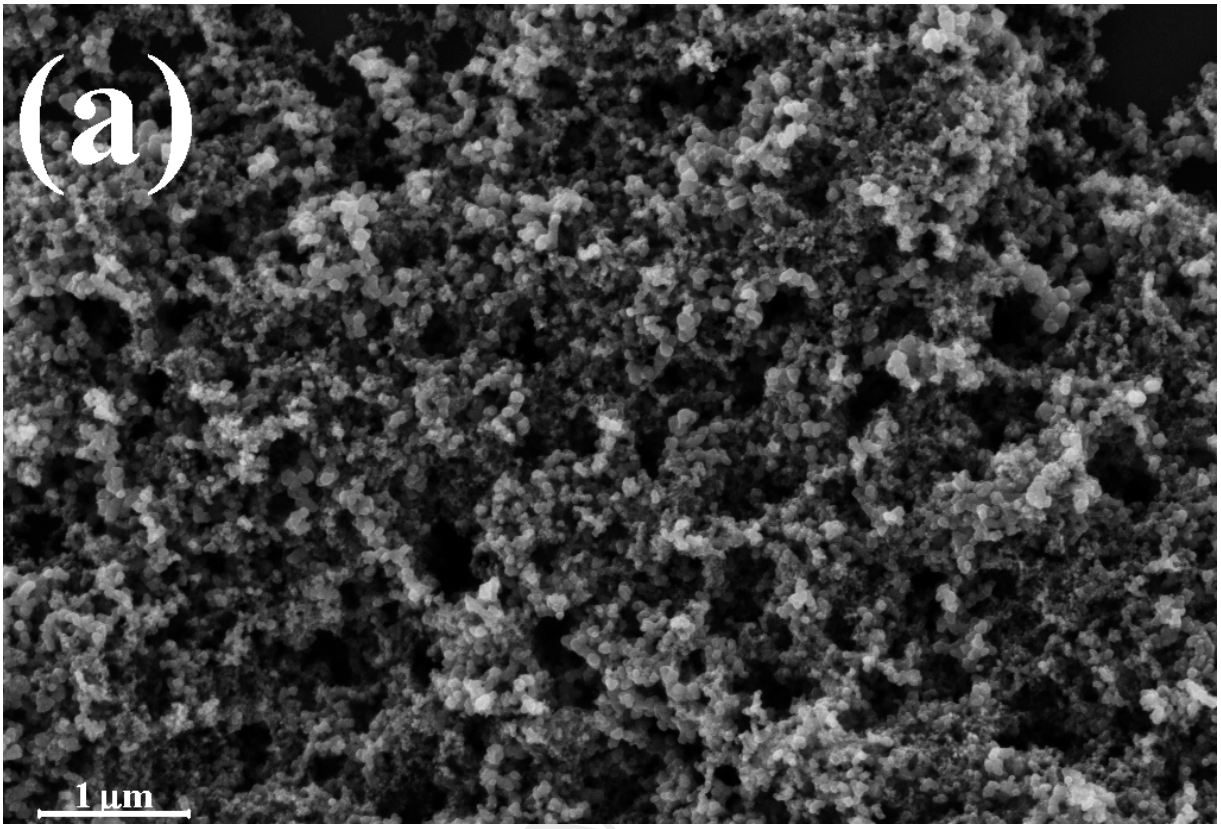

Fig 3 (a) .

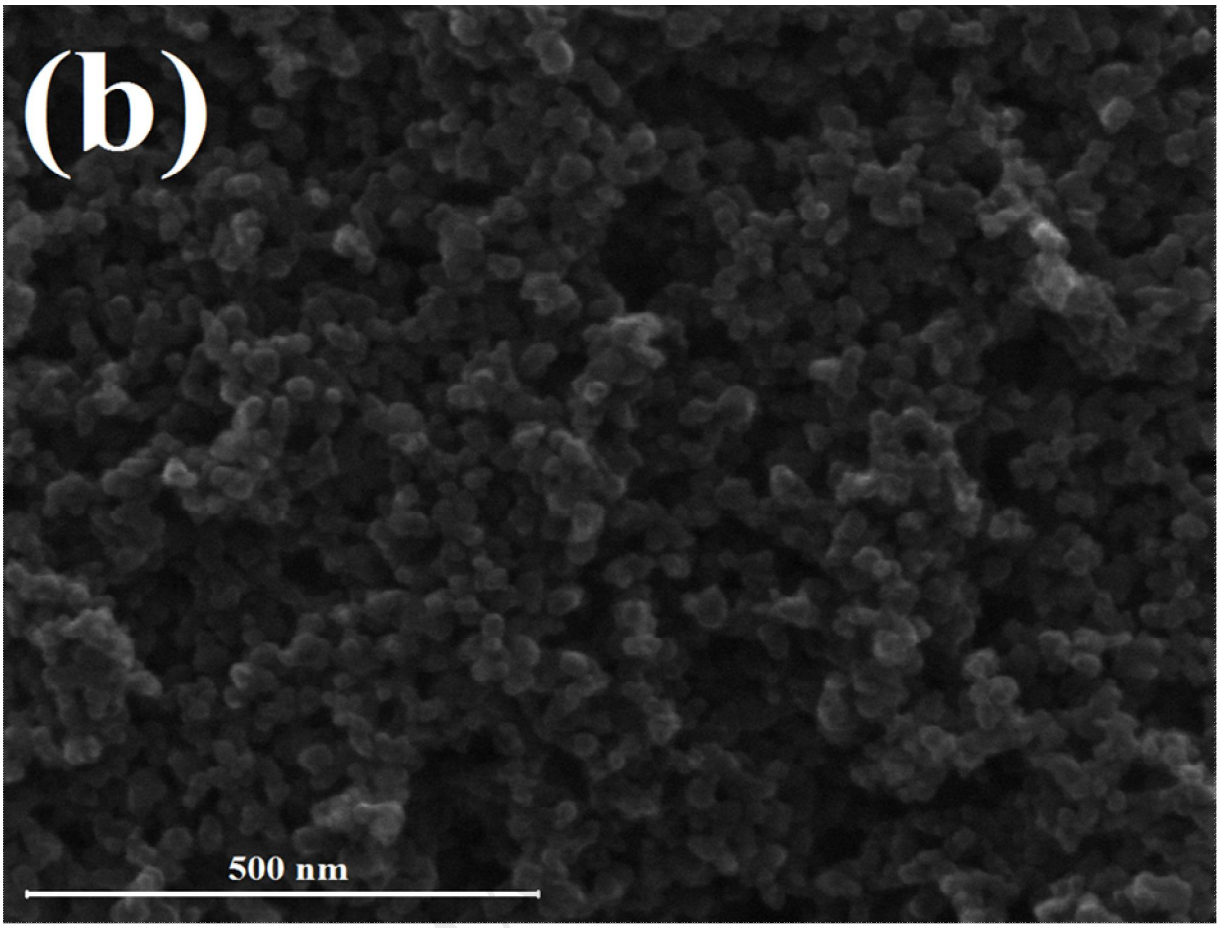

Fig 3 (b) .

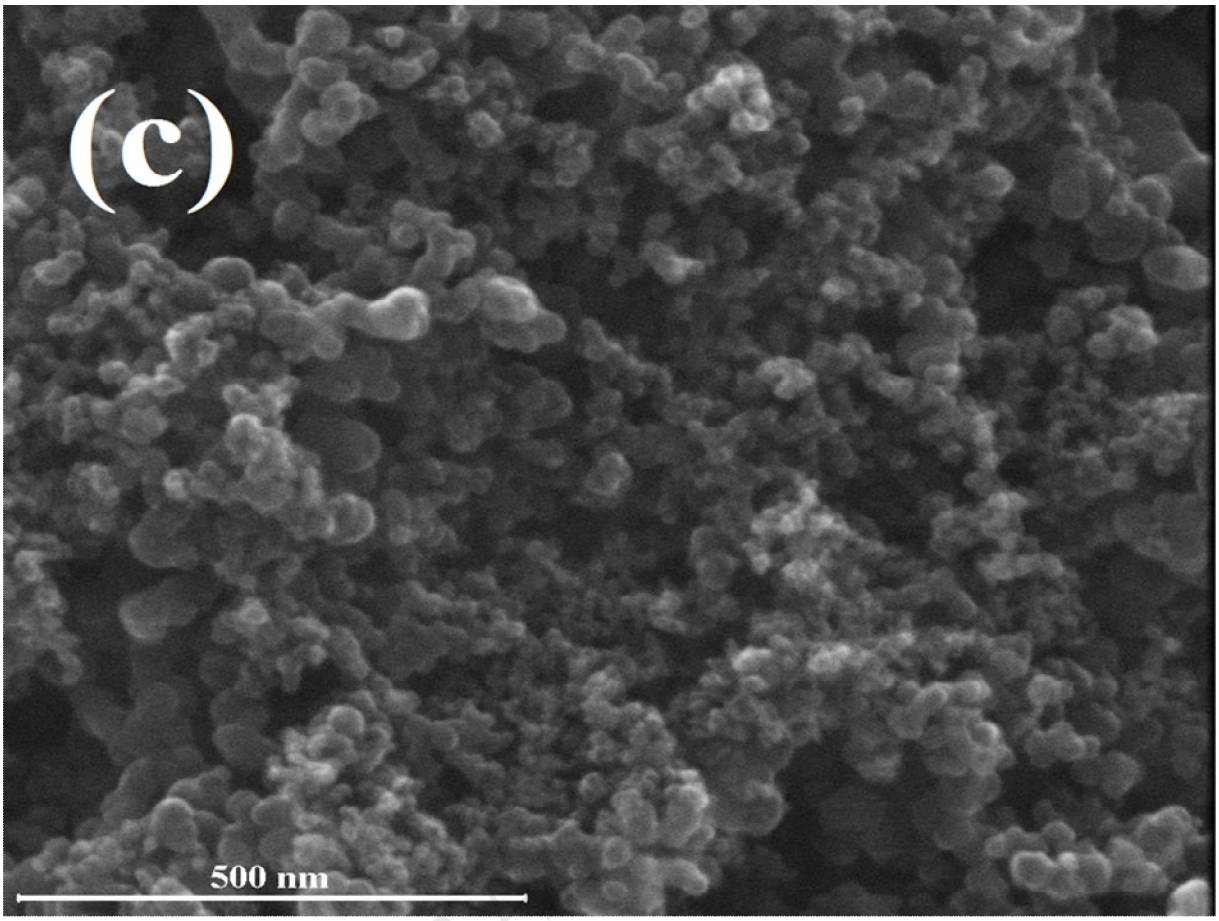

Fig 3 (c) .

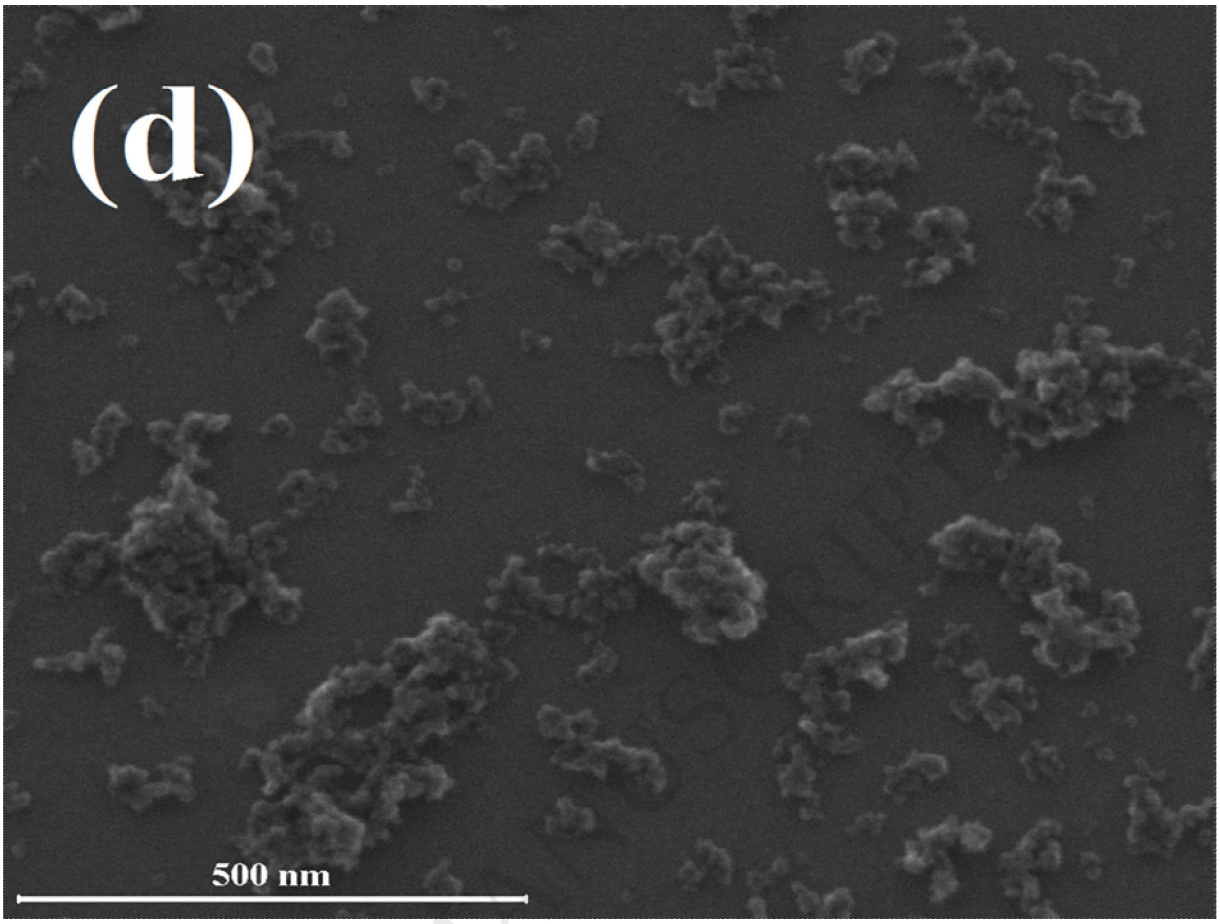

Fig 3 (d) .

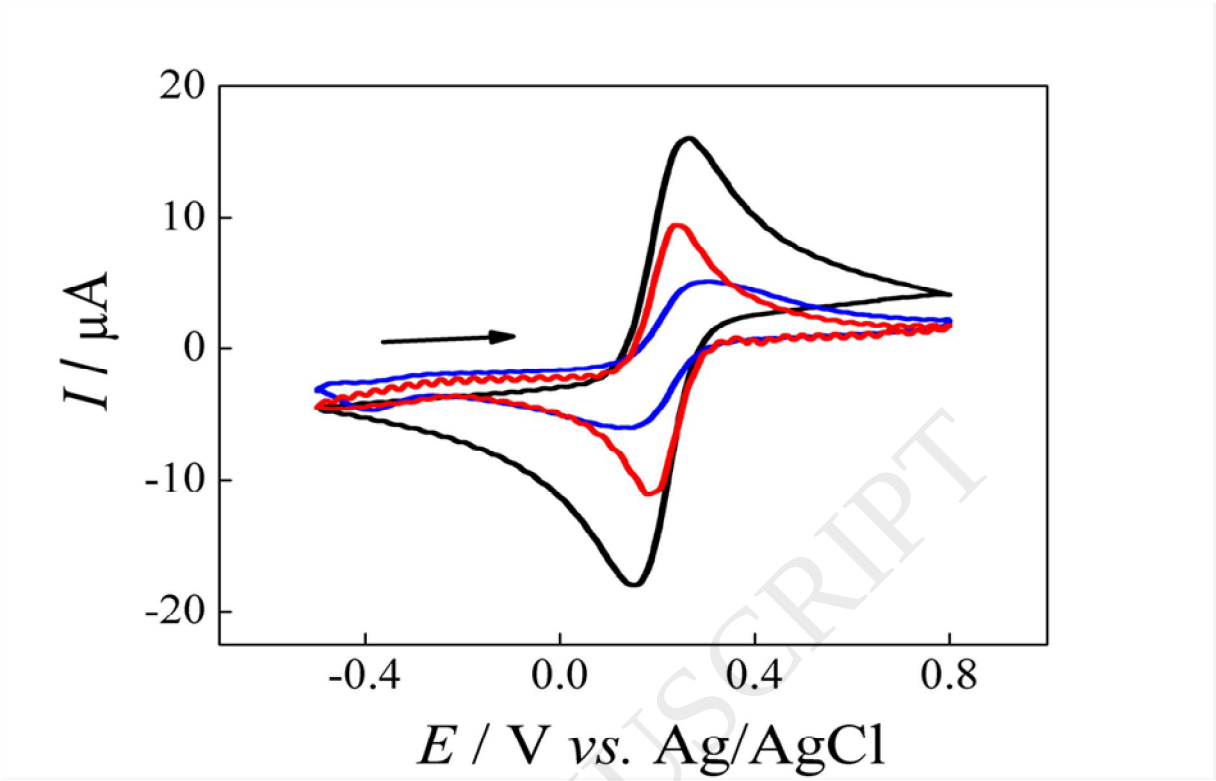

Fig 4 .

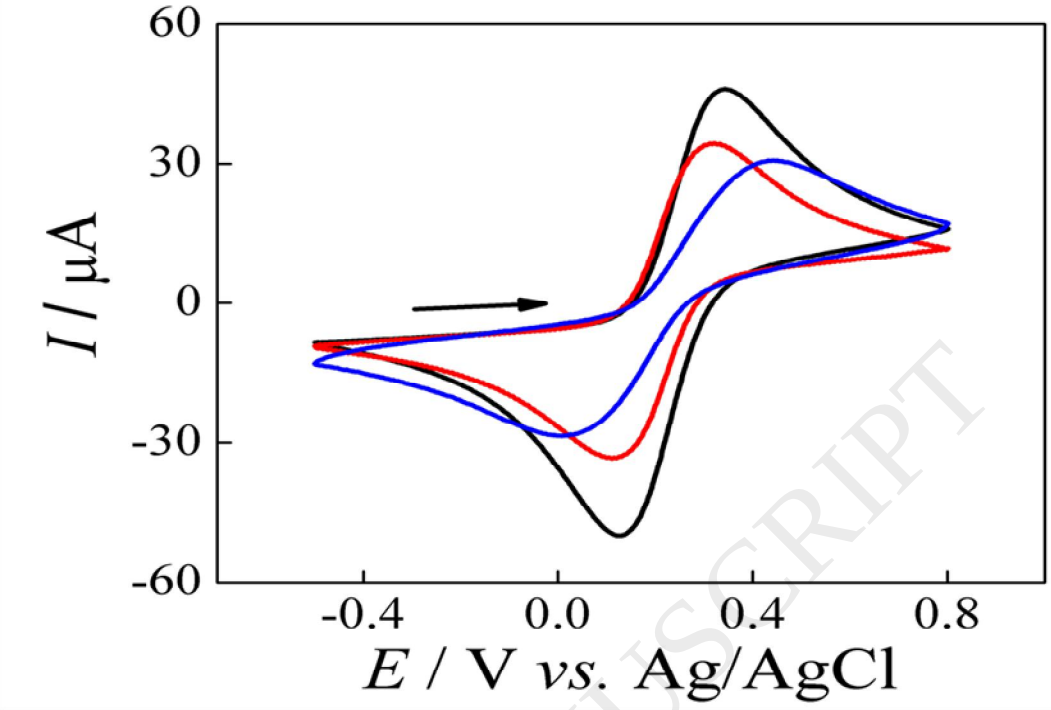

Fig 5 .

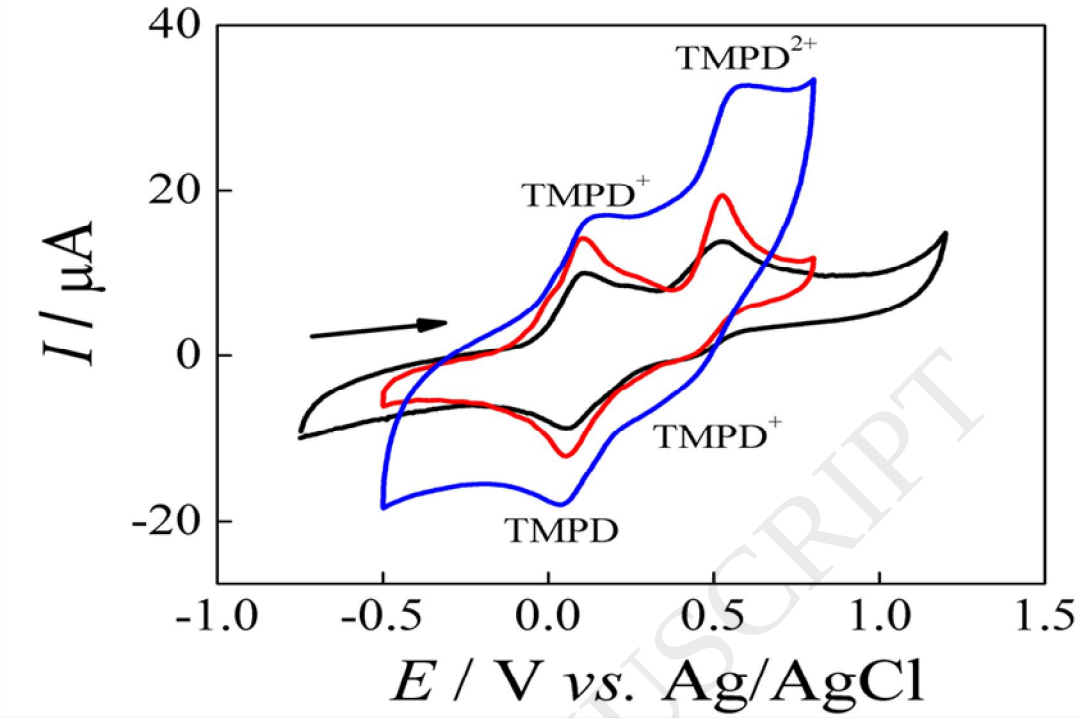

Fig 6 .

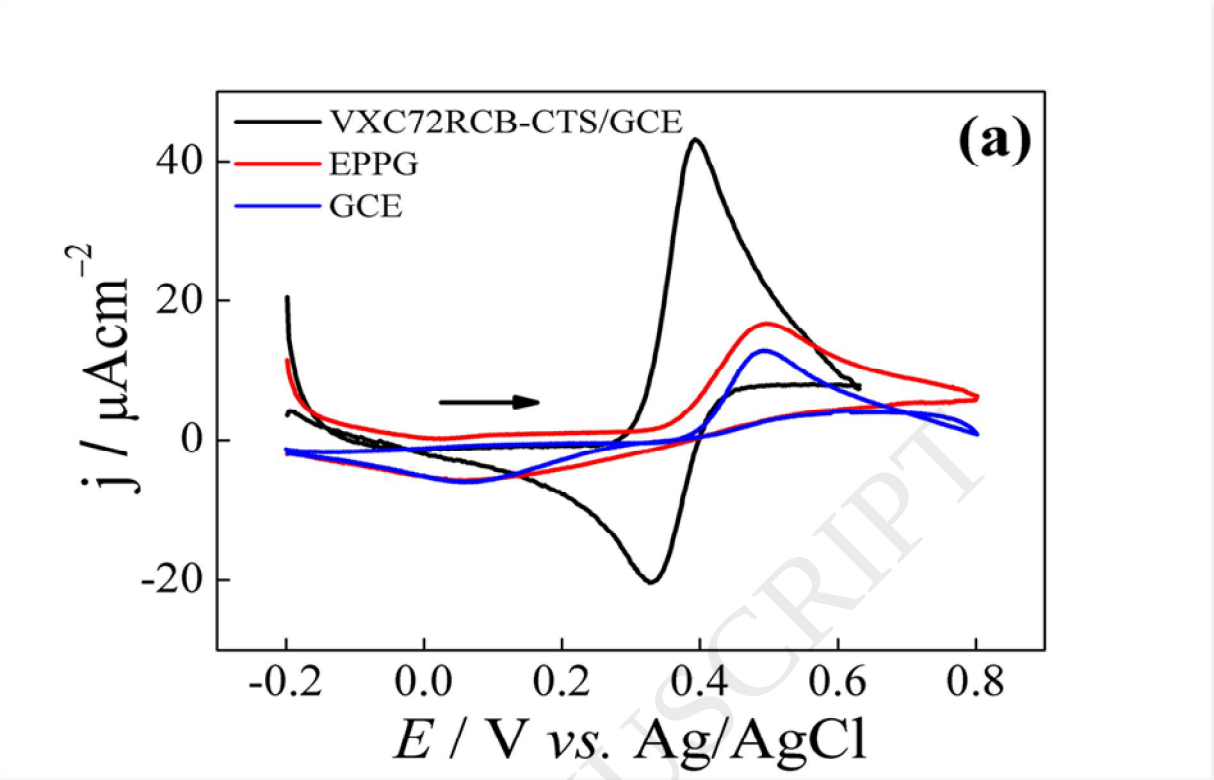

Fig 7 (a) .

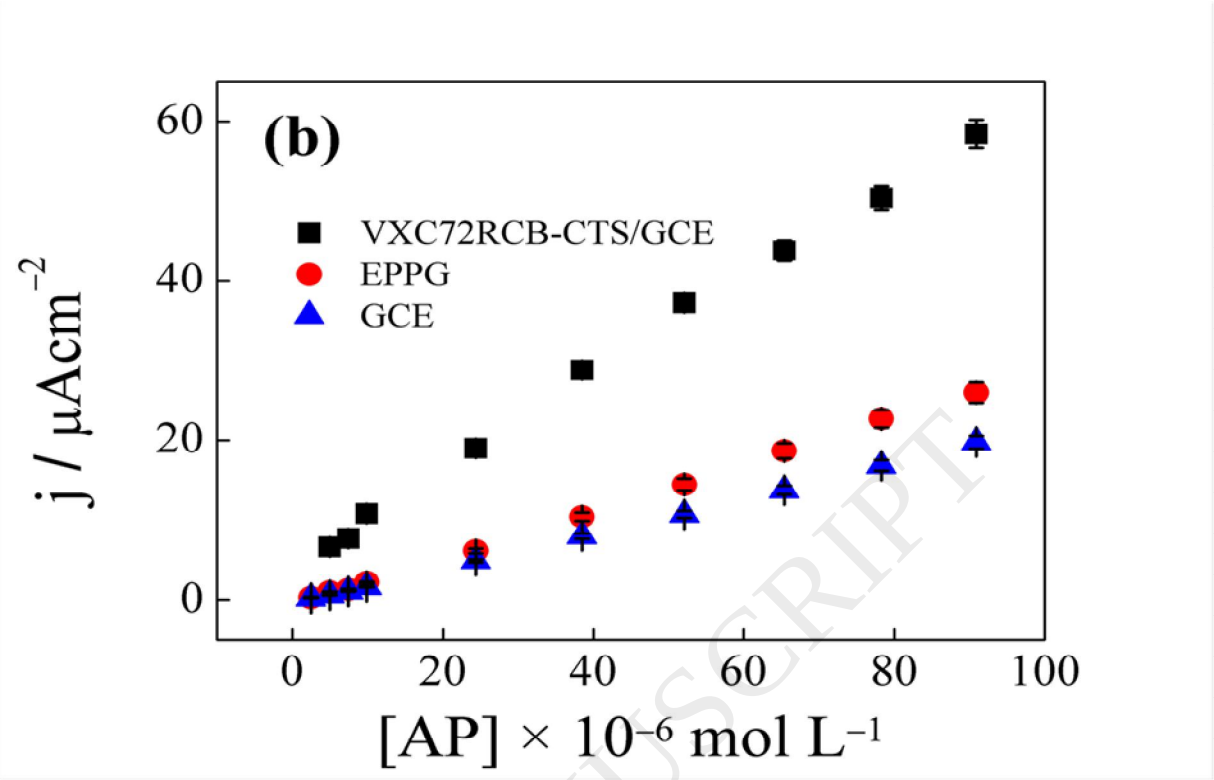

Fig 7 (b) .

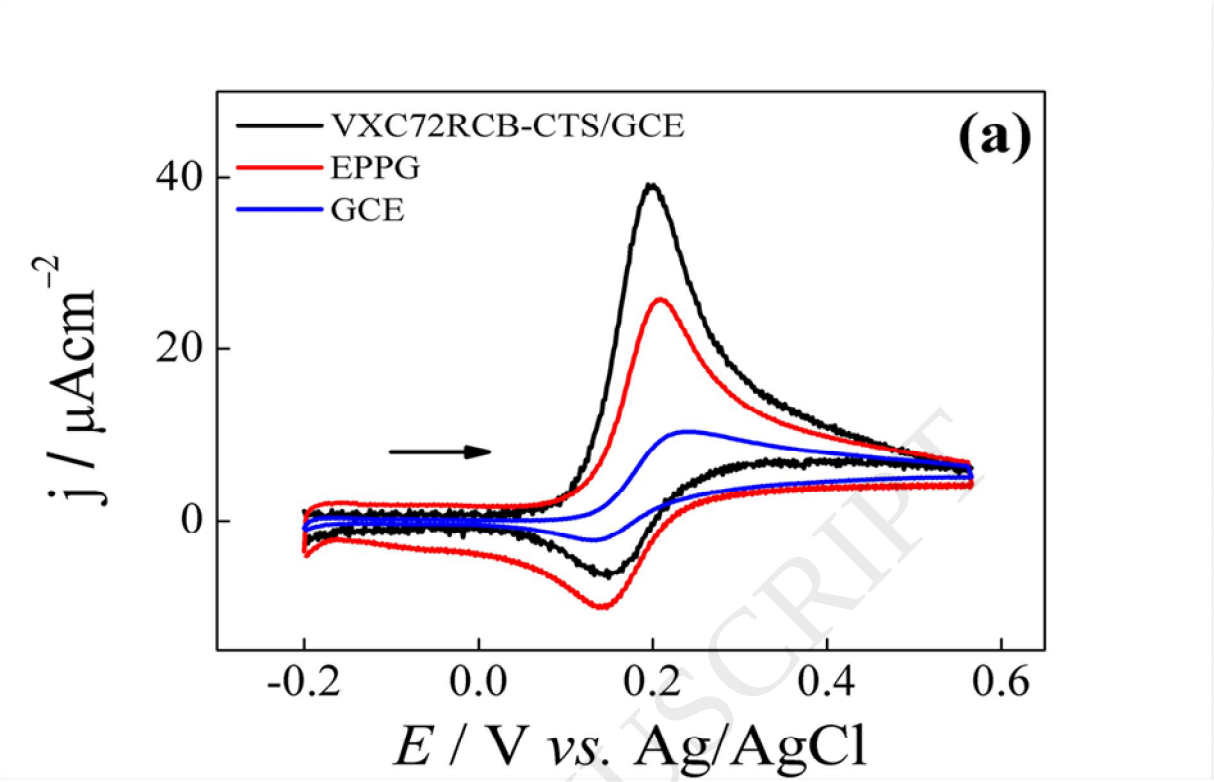

Fig 8 (a) .

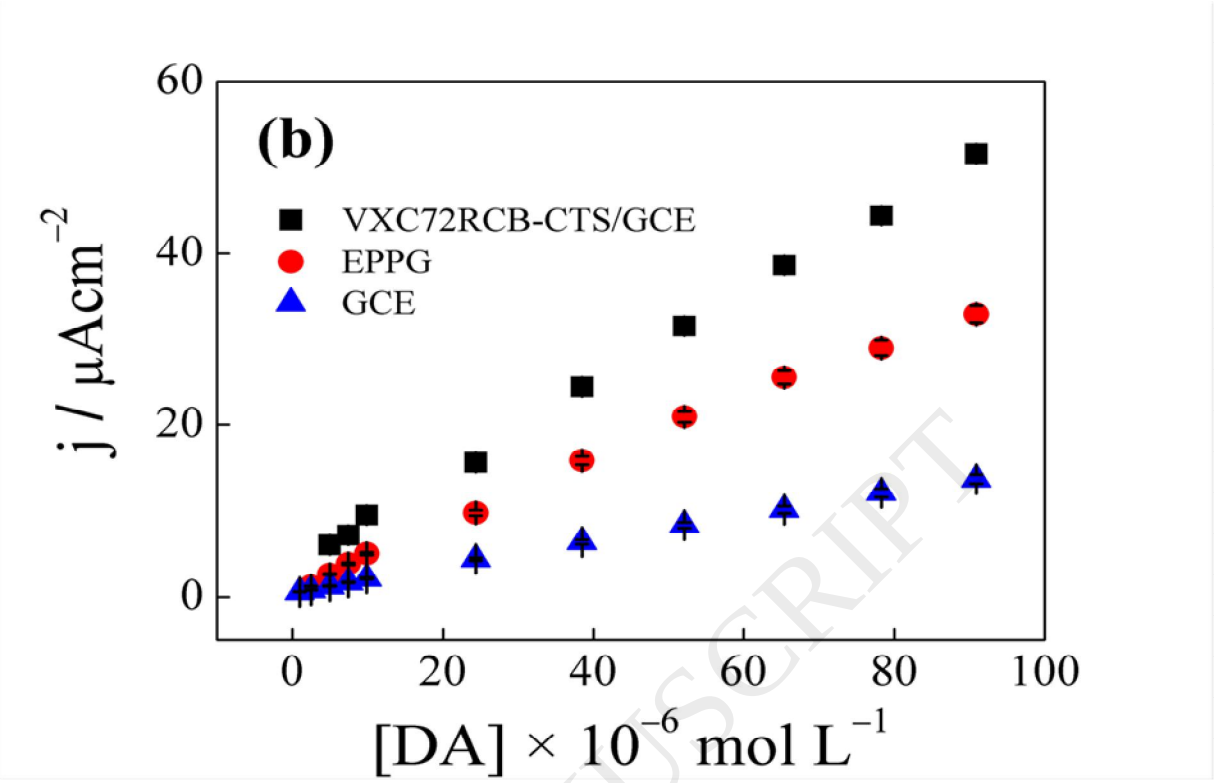

Fig 8 (b) .

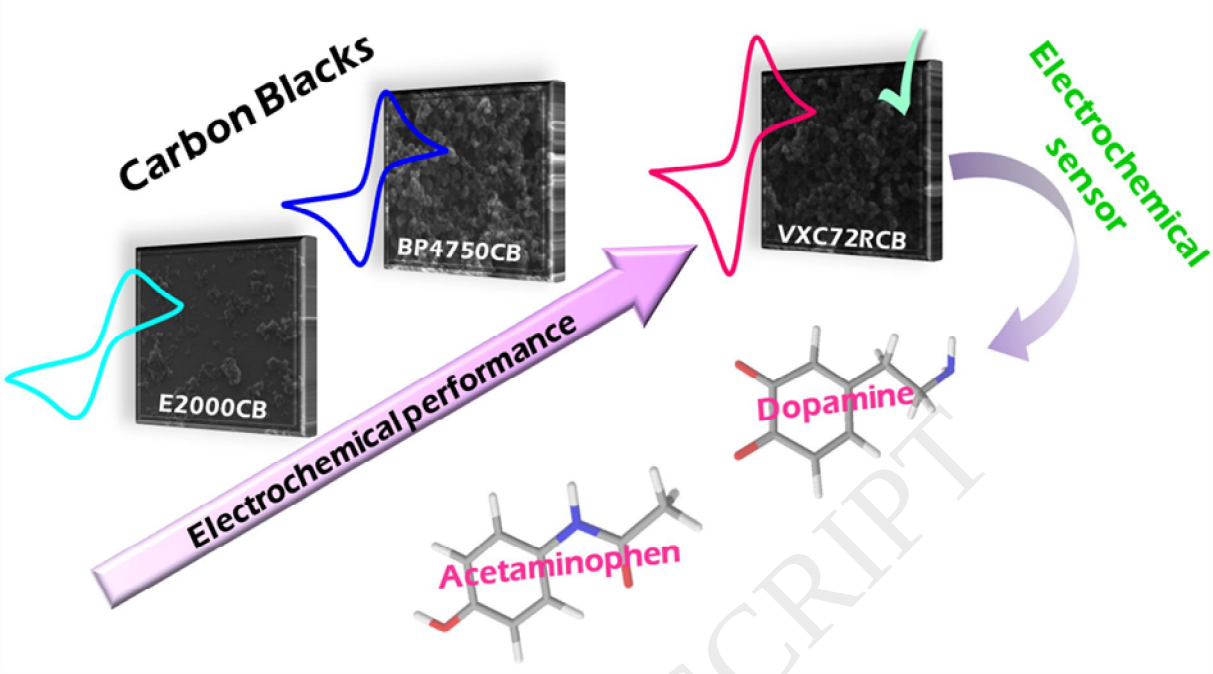

Graphical Abstract .